RESEARCH PAPER

Different profiles of Ca^{2+} responses to endothelin-1 and PDGF in liver myofibroblasts during the process of cell differentiation

N Kojima, M Hori, T Murata, Y Morizane and H Ozaki

Department of Veterinary Pharmacology, Graduate School of Agriculture and Life Sciences, The University of Tokyo, Bunkyo-ku, Tokyo, Japan

Background and purpose: Hepatic stellate cells play an important role in liver fibrosis but little is known about liver myofibroblasts located around the central vein and in the portal area. In this study, intracellular Ca^{2+} concentration ($[Ca^{2+}]_i$) was measured to assess the response to endothelin-1 (ET-1), platelet derived growth factor (PDGF) and ATP in rat liver myofibroblasts.

Experimental approach: Rat liver myofibroblasts were compared in 'quiescent' (cultured on Matrigel-coated dishes) and 'activated' (cultured on non-coated plastic dishes) conditions. $[Ca^{2+}]_i$ was measured with the fluorescent dye fura-2 and mRNA for ET-1, PDGF and their receptors by RT-PCR.

Key results: ET-1 increased $[Ca^{2+}]_i$ in quiescent cells but not in activated cells, whereas PDGF-BB increased $[Ca^{2+}]_i$ in activated cells but not in quiescent cells. However, there was no difference between responses to ATP in quiescent or activated cells. ET-1 (in quiescent cells), PDGF-BB (in activated cells) and ATP (in both cells) all induced transient increases in $[Ca^{2+}]_i$ in the absence of extracellular Ca^{2+} (with EGTA), indicating the involvement of Ca^{2+} release from intracellular Ca^{2+} stores. The sustained increase in $[Ca^{2+}]_i$ in the presence of external Ca^{2+} in activated cells (ATP and PDGF) was significantly reduced by nicardipine, a L-type Ca^{2+} channel blocker, but not in quiescent cells (ATP and ET-1).

Conclusions and implications: The different pharmacological profiles of $[Ca^{2+}]_i$-response in quiescent and activated myofibroblasts suggest that ET-1 and PDGF contribute differently to myofibroblast activation during the process of liver fibrosis.

Introduction

Fibrosis, defined pathologically as inappropriate repair by connective tissue, is increasingly recognized as an important feature of many chronic diseases. Traditionally, fibrosis has been viewed as the irreversible, end-stage sequel to a multitude of diverse disease processes. The lack of effective treatments, the high mortality and the increasing morbidity attributed to chronic fibrotic diseases has stimulated an explosion of research into cellular, molecular and genetic aspects of liver fibrosis. With on-going liver damage, the imbalance between matrix synthesis and matrix degradation together with hepatocellular necrosis leads to liver fibrosis, which is considered to be reversible, and then finally to liver cirrhosis, which is considered irreversible. Therefore, prevention of liver fibrosis progression to liver cirrhosis is the major clinical target of therapy.

Hepatocytes are the parenchymal cells of the liver, which comprise over 60% of the liver cell mass. The non-parenchymal cells include liver macrophages (Kupffer cells), sinusoidal endothelial cells, hepatic stellate cells (HSC), biliary cells and (myo)fibroblasts. In the case of liver fibrosis, myofibroblasts and myofibroblast-like cells, which are activated upon liver injury, are the main suppliers of the extracellular matrix. A large number of studies have provided evidence that HSCs become myofibroblast-like when activated and it has long been thought that HSC-derived myofibroblast-like cells are the key players in liver fibrosis. However, there are other cell types of the fibroblast lineage,

Correspondence: Dr H Ozaki, Department of Veterinary Pharmacology, Graduate School of Agriculture and Life Sciences, The University of Tokyo, Yayoi 1-1-1, Bunkyo-ku, Tokyo 113-8657, Japan.
E-mail: aozaki@mail.ecc.u-tokyo.ac.jp

in particular the liver (myo)fibroblasts located around the central vein and in the portal area, which also play a role in liver fibrosis (Knittel *et al.*, 1999; Saile *et al.*, 2002). In response to hepatic wounding, these (myo)fibroblasts also undergo activation, and produce increased quantities of extracellular matrix proteins, proliferate and migrate (Kinnman *et al.*, 2003).

Isolated HSCs do not proliferate and therefore cannot be passaged after isolation. In contrast, isolated rat liver myofibroblasts can be subcultivated at least up to the 10th passage. HSC-derived myofibroblast-like cells and myofibroblasts show differences in expression of fibulin 2, P100 and interleukin-6 (Knittel *et al.*, 1999; Ramadori and Saile, 2002). Beside the importance of the activation of HSCs in liver fibrosis and cirrhosis, the involvement of portal tract (myo)fibroblasts around biliary structures has now been clearly demonstrated (Ramadori and Saile, 2002; Desmoulière *et al.*, 2003; Pinzani and Rombouts, 2004; Novo *et al.*, 2006).

There is mounting evidence indicating that endothelin-1 (ET-1) is an important factor in liver fibrosis (Hui and Friedman, 2003; Bataller and Brenner, 2005; Muddu *et al.*, 2007). ET-1 expression is markedly enhanced in cirrhotic liver tissue (Pinzani *et al.*, 1996), and the peptide is overproduced by HSCs during liver injury (Rockey *et al.*, 1998). It has also been reported that ET-1 exerts several actions on HSCs, including mitogenicity, activation of MAP kinase and reversible cell contraction (Thimgan and Yee, 1999), all of which appear to be mediated by ET_A receptors (Pinzani *et al.*, 1996; Reinehr *et al.*, 1998). Stimulation of migration by ET-1 has also been reported (Kinnman *et al.*, 2000; Tangkijvanich *et al.*, 2001). The role of ET-1 in both microcirculation and the pathophysiology of portal hypertension has also been proposed (Reynaert *et al.*, 2002). On the other hand, with serial subculture, the predominance of ET receptors changes from subtype A to subtype B (Pinzani and Rombouts, 2004). ET_B stimulation activates the cAMP pathway and inhibits proliferation (Mallat *et al.*, 1996; Reinehr *et al.*, 2002).

In rat and human fibrotic liver, expression of platelet-derived growth factor (PDGF) and its receptor has been shown to be increased in experimental fibrosis. PDGF has also been identified as the most potent growth factor to stimulate the proliferation (Pinzani *et al.*, 1989; Kinnman *et al.*, 2001; Pinzani and Rombouts, 2004) and the migration (Kinnman *et al.*, 2000; Tangkijvanich *et al.*, 2002) of culture-activated HSCs. Moreover, it has been reported that PDGF-B overexpression in transgenic mice causes HSC and myofibroblast activation (Czochra *et al.*, 2006).

Because the accumulation of extracellular matrix observed in hepatic fibrosis is due to the activation of HSCs and liver (myo)fibroblasts, which acquire a myofibroblastic phenotype, it is important to determine the changes in pharmacological properties during the process of myofibroblastic conversion. In addition, it is widely accepted that intracellular Ca^{2+} regulates various cellular responses in fibroblasts, including proliferation, cell growth, migration, cell adhesion, apoptosis, gene transcription and contraction. However, only few studies have examined Ca^{2+} signalling in HSCs, with even fewer looking at liver myofibroblasts.

In the present study, intracellular Ca^{2+} concentration ($[Ca^{2+}]_i$) was measured in liver myofibroblasts to assess the response to several fibrogenic factors, such as ET-1, PDGF-BB and adenosine 5′-triphosphate (ATP), and the results were compared in quiescent and activated states. The data show that the profiles of changes in $[Ca^{2+}]_i$ due to ET-1 and PDGF are different in quiescent and activated cells, indicating the different contributions of these factors during the process of liver fibrosis.

Materials and methods

Cell culture and isolation

Rat myofibroblasts were isolated from male Sprague–Dawley rats with an average body weight between 350 and 400 g. Ethylene glycol bis(β-aminoethylether)-N,N,N',N'-tetraacetic acid (EGTA) was dissolved in a buffer containing 137 mM NaCl, 5.37 mM KCl, 0.57 mM NaH$_2$PO$_4$/2H$_2$O, 0.34 mM Na$_2$HPO$_4$/12H$_2$O, 0.42 mM NaHCO$_3$, 10 mM HEPES and 5 mM glucose (Wako, Osaka, Japan). Pronase E, collagenase and DNase I were dissolved in a standard buffer containing 137 mM NaCl, 5.37 mM KCl, 6.8 mM CaCl$_2$, 0.57 mM NaH$_2$PO$_4$/2H$_2$O, 0.34 mM Na$_2$HPO$_4$/12H$_2$O, 0.42 mM NaHCO$_3$, 10 mM HEPES and 5 mM glucose (Wako). In brief, the liver was perfused with 0.5 mM EGTA solution for 3 min to wash out the blood, and then dispersed by perfusion with 0.67 mg ml^{-1} pronase E (Merck, Darmstadt, Germany) for 6 min and then with 0.33 mg ml^{-1} collagenase (Wako) for 6 min. Next, the liver was dissected from the body and placed in a dish containing 0.5 mg ml^{-1} collagenase, 0.5 mg ml^{-1} pronase E and 0.01 mg ml^{-1} DNase I (Roche, Basel, Switzerland), and minced. The tissue samples were then incubated with stirring, for 15 min at 37°C. The digested liver was filtered through sterile mesh screen (Sigma-Aldrich Japan, Tokyo, Japan, Cell Dissociation Sieve Kit) and the resulting cell suspension was centrifuged at 50 g for 1 min at 4°C to separate non-parenchymal cells and hepatocytes. The non-parenchymal cell fraction was centrifuged at 700 g for 7 min at 4°C and then the pellet was suspended in GBSS (Gey's Balanced Salts Solution) containing 15% Nycodenze (Histodenz, Sigma-Aldrich Japan). The non-parenchymal cells were separated using the density gradient centrifugation method. The cell solution was double layered with 2 ml of 8.5% Nycodenz solution and centrifuged for 20 min at 1200 g at 4°C. The cell fraction in the top 3 ml was collected and washed with GBSS, and then plated. Cells were supplemented with 10% fetal bovine serum (JRH Biosciences, Lenexa, KS, USA), and incubated at 37°C in a humidified atmosphere. They were passaged 3–5 times and starved overnight before use. The rat liver myofibroblasts were purified and obtained by outgrowth from other non-parenchymal cells. The medium was changed every 3 days. Cells were starved overnight before experimentation. To culture cells on Matrigel (BD Biosciences, Franklin Lakes, NJ, USA), a Matrigel gel layer (0.3–0.5 mm) was mounted on a glass cover slip, incubated at 37°C for 30 min to solidify and passaged liver myofibroblasts were seeded on the surface of the gel.

[Ca^{2+}]$_i$ measurement
Cells were incubated in a solution containing (in mM) 137 NaCl, 5.4. KCl, 11.5 glucose, 1.5 CaCl$_2$, 1.2 MgCl$_2$ and 10 HEPES. [Ca^{2+}]$_i$ was measured using fura-2 AM. Myofibroblasts were cultured on glass coverslips and measured when confluent. Cells (days 2–5) were starved overnight before measurement. Cells were loaded with 5 μM fura-2AM for 45 min at 37°C. Every 3 s, the fluorescence of an image at 340 nm (F340) was divided by the fluorescence of an image at 380 nm (F380) to provide a resultant ratio (F340/F380) by means of a fluorescence imaging system (Hamamatsu Photonics, Hamamatsu, Japan). To remove extracellular Ca^{2+}, Ca^{2+}-free HEPES-buffered solution (containing 0.5 mM EGTA instead of 1.5 mM CaCl$_2$) was used. The area under the Δratio per time curve (AUC) was calculated to assess the response.

Actin staining
Cells cultured on glass slips with Matrigel and on non-coated plastic were fixed in 4% formaldehyde for 10 min at 37°C with stirring, and then incubated with 0.1% Triton for 1 min. Cells were blocked with 5% skim milk for 30 min at 37°C. Cells were then incubated with a 1:100 dilution of anti-α-actin IgG (Dako, Glostrup, Denmark) for 1 h and then incubated with a 1:100 dilution of Alexa Fluor 594 phalloidin (Invitrogen Japan, Tokyo, Japan) and a 1:100 dilution of FITC-conjugated anti-mouse IgG antibodies (Vector Laboratory, Burlingame, CA, USA) for 1 h. Cells were finally incubated with 1 μg ml^{-1} of DAPI (Sigma) for 5 min.

Reverse-transcription polymerase chain reaction
To investigate the presence of receptor transcripts in rat myofibroblasts, total RNA was extracted from cells cultured on Matrigel and non-coated plastic dishes using the acid guanidinium thiocyanate-phenol-chloroform method employing the TRIzol Reagent (Invitrogen Japan). RNA concentration and purity were determined using a ND-1000 Spectrophotometer (Nano Drop, Wilmington, DE, USA). First-strand cDNA was synthesized using a random 9-mer primer and avian myeloblastosis virus reverse transcriptase XL at 30°C for 10 min, 55°C for 90 min, 99°C for 5 min and 4°C for 5 min. Polymerase chain reaction (PCR) was performed using Taq DNA polymerase (Ampli Taq Gold) and synthetic gene-specific primers for glyceraldehyde-3-phosphate dehydrogenase (GAPDH), α-smooth muscle actin (α-SMA), prepro ET-1, PDGF-A, PDGF-B, ET$_A$ receptor, platelet-derived growth factor receptor-α (PDGFR-α) and PDGFR-β. The forward and reverse primers were as follows: rat GAPDH (expected product size 308 bp: X00972) 5′-TCCCTCAAGATTGTCAGCAA-3′ (forward), 5′-AGATCCACAACGGATACATT-3′ (reverse); α-SMA (303 bp: XM_001079913.1) 5′-GTGGCTATTCAGGCTGTGCT-3′ (forward), 5′-AGAAGAGGAAGCAGCAGTGG-3′ (reverse); prepro ET-1 (368 bp: NM_012548.1) 5′-TCTCTGCTGTTTGTGGCTTTC-3′ (forward), 5′-TCGGAGTTCTTTGTCTGTTTG-3′ (reverse); PDGF-A (226 bp: NM_012801.1) 5′-CCTGTGCCCATCCGCAGGAAGAGA-3′ (forward), 5′-TTGGCCACCTTGACACTGCGGTG-3′ (reverse); PDGF-B (434 bp: XM_343293.3) 5′-CATCCGCTCCTTTGATGAC-3′ (forward), 5′-GTCTCACAC

TTGCAGGCCAG-3′ (reverse); ET$_A$ (205 bp: NM_012550.1) 5′-ATGAGATGGATAAGAACC-3′ (forward), 5′-CCATTCATGGGGACCCAGG-3′ (reverse); PDGFR-α (164 bp: XM_214030.3) 5′-TCTCGGCATGACGGATTCTT-3′ (forward), 5′-CCACACTGAAGGTTCCGTTGA-3′ (reverse); and PDGFR-β (677 bp: NM_031525.1) 5′-CAACATTTCGAGCACCTTTGT-3′ (forward), 5′-AGGGCACTCCGAAGAGGTAA-3′ (reverse). PCR amplification was tried at 30, 33, 35, 37 and 38 cycles and optical band density was compared. We chose 35 cycles, where it was most linear and acceptable for quantification. After denaturation at 95°C for 10 min, 35 cycles of amplification were performed at 95°C for 0.4 min, 56°C for 1 min and 72°C for 1 min using a thermal cycler (Takara PCR Thermal Cycler MP, Takara Bio Inc., Shiga, Japan). PCR products were electrophoresed through 2% agarose gel containing 0.1% ethidium bromide. Electrophoresis was performed at 100 V for 35 min and detectable fluorescent bands were visualized using a UV transilluminator. The densitometric intensity was quantified using Scion Image beta 4.02 analysis software (Frederick, MD, USA). All primers were designed to sandwich exons (except for PDGFR-α) and lack of genomic contamination was confirmed by the fact that there were only single bands which were in accordance with predicted product size. For PDGFR-α, we confirmed lack of genomic contamination by comparing the result from reactions with and without reverse transcriptase. Results are expressed as the percentage of optical band density $\pm$ s.e.m. relative to GAPDH.

Statistical analysis
The data are expressed as the mean $\pm$ s.e. Statistical evaluation of the data was performed by unpaired Student's *t*-test for comparison between two groups. Statistical significance was established at the $P < 0.05$ level (*$P < 0.05$ and **$P < 0.01$).

Materials
The chemicals used were BQ-123 (Calbiochem, Darmstadt, Germany), nicardipine hydrochloride (Sigma), ionomycin calcium salt (Sigma-Aldrich, USA), endothlin-1 (ET-1) (Human, Peptide Institute Inc., Osaka, Japan), sarafotoxin S6c (Peptide Institute), ATP disodium salt (Sigma-Aldrich), platelet-derived growth factor-BB (PDGF-BB) (Rat, Sigma-Aldrich), 2-aminoethyl diphenylborinate (2-APB) (Lancaster Synthesis, Eastgate, White Lund, Morecambe, England), Bay K8644 (Sigma-Aldrich), gadolinium chloride hexahydrate (Wako), thapsigargin (Sigma-Aldrich) and growth factor-reduced Matrigel Matrix w/o Phenol Red (BD Biosciences).

Results

Morphological features and expression of α-smooth muscle actin (α-SMA) in cultured myofibroblasts
Basement membranes are thin extracellular matrices underlying cells *in vivo* and the Matrigel medium we have used is a soublized preparation of basement membrane. Culturing myofibroblasts on Matrigel can reverse the activation process (Sohara *et al.*, 2002). It has also been reported that HSCs are able to maintain their quiescent phenotype when cultured on Matrigel or within a collagen gel (Friedman *et al.*, 1989;
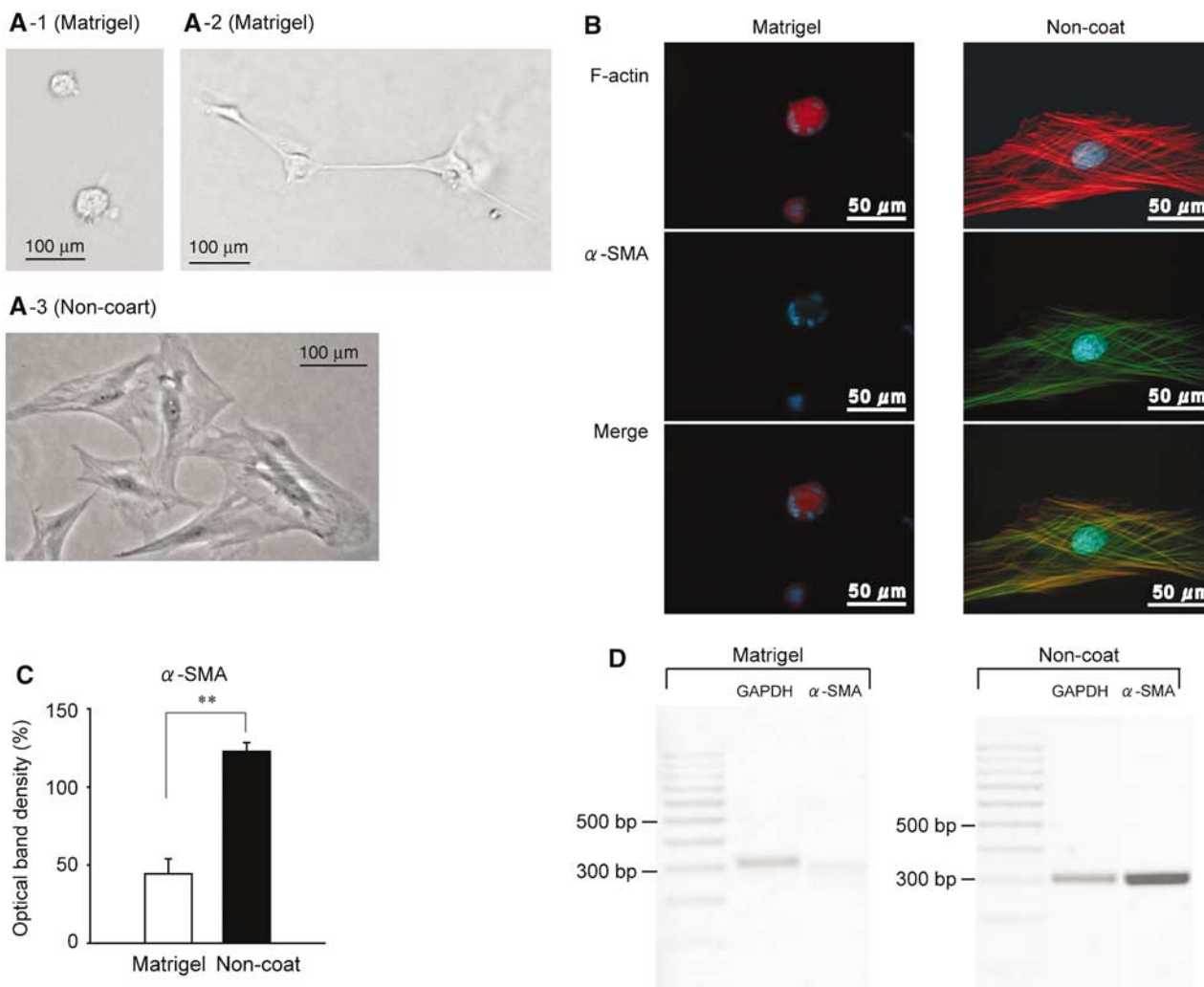
Figure 1 Activated myofibroblasts (cultured on plastic) expressed greater amounts of α-smooth muscle actin (α-SMA). Myofibroblasts were cultured on either Matrigel or non-coated plastic dishes and starved overnight. (**A**) (1: cultured at low density; 2: cultured at high density) Matrigel-cultured rat liver myofibroblasts, and (**C**) non-coated plastic-cultured rat liver myofibroblasts. (**B**) Left: Matrigel-cultured rat liver myofibroblasts and (**B**) (right) shows non-coated plastic-cultured rat liver myofibroblasts stained with F-actin and α-SMA (top, F-actin; middle, α-SMA; bottom, F-actin and α-SMA merged). (**C**) and (**D**) show α-SMA mRNA expression assessed by semi-quantitative reverse-transcription polymerase chain reaction (RT-PCR) ($n = 5–6$). Results are expressed as the percentage of optical density $\pm$ s.e.m. relative to glyceraldehyde-3-phosphate dehydrogenase (GAPDH). **$P < 0.01$.

Senoo *et al.*, 1996). We applied this technique to rat liver myofibroblasts.

Cells cultured on Matrigel had a ball-like appearance when cells were seeded at low density (Figure 1A-1) or formed clusters that were occasionally connected by a filamentous network when the cells were seeded at high density (Figure 1A-2). Cells cultured on non-coated plastic were spread out and flattened (Figure 1A-3). This change in morphology was induced only when cells were cultured on Matrigel and not when cells were cultured on a collagen-coated dish (cell matrix collagen Type I-A, Nitta Gelatin, Osaka, Japan) (data not shown).

When myofibroblasts including HSCs and liver myofibroblasts are activated, they express greater amounts of α-SMA (Olaso and Friedman, 1998; Desmouliere *et al.*, 2003; Kinnman *et al.*, 2003; Ramadori and Saile, 2004; Carpino *et al.*, 2005). Activation of myofibroblasts was confirmed by reverse-transcription (RT)-PCR and immunocytochemistry with specific antibodies. Activated myofibroblasts (cultured on non-coated plastic dishes) expressed greater amounts of α-SMA (Figure 1B). In activated myofibroblasts, the expression of α-SMA was intense and distributed along the numerous stress fibers. However, in quiescent myofibroblasts, F-actin was distributed evenly and stress fibers could not be seen. In addition, the purity of isolated primary culture cells that were passaged 3–5 times and cultured on non-coated plastic was confirmed, because all cells that stained with phalloidin F-actin also expressed α-SMA. In accordance with the immunocytochemistry, mRNA expression of α-SMA was 2.7 times higher in non-coated-cultured cells than in Matrigel-cultured cells (Figure 1C and D).

Therefore, in this study, we assumed that Matrigel-cultured cells and non-coated plastic-cultured cells reflect quiescent and activated myofibroblasts, respectively.
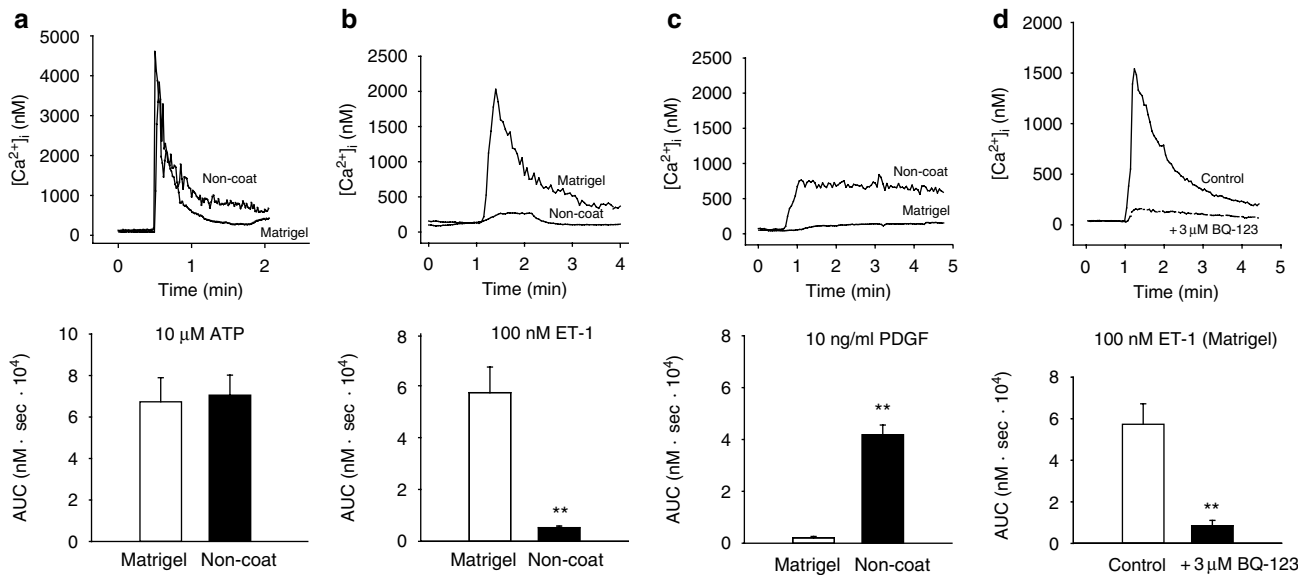
Figure 2 Matrigel- and non-coated plastic-cultured cells responded differently to endothelin-1 (ET-1) and platelet-derived growth factor (PDGF). Myofibroblasts were cultured on either Matrigel or non-coated plastic dishes and starved overnight. Changes in intracellular Ca^{2+} concentration ($[Ca^{2+}]_i$) were measured using Ca^{2+} fluorescent dye fura-2. Results are shown as the area under the $[Ca^{2+}]_i$-time curve (AUC: 0–2 min) for 100 μM adenosine 5'-triphosphate (ATP) (**a**), 100 nM ET-1 (**b**) and 10 ng ml^{-1} PDGF (**c**). Cells were pretreated with 3 μM BQ-123 for 3 min before stimulation with ET-1 in (**d**). Data are presented as mean$\pm$s.e.m. of 17–43 cells from 4–5 separate experiments. **$P < 0.01$.

$[Ca^{2+}]_i$ responses to ET-1 and PDGF-BB

We examined the effect of ET-1 and PGDF-BB on $[Ca^{2+}]_i$, comparing the effects between quiescent myofibroblasts (Matrigel) and activated myofibroblasts (non-coated). We also examined the effect of ATP, because purinergic agonists also contribute to fibroblast activation (Harada *et al.*, 2000; Dranoff *et al.*, 2004). ATP (10 μM) induced a transient increase in $[Ca^{2+}]_i$ which then gradually decreased to a level above the resting level (sustained phase). The amplitude of the transient $[Ca^{2+}]_i$ increase induced by ATP in the quiescent cells was comparable to that in the activated cells (Figure 2a). ET-1 (100 nM) also induced biphasic increases in $[Ca^{2+}]_i$ in quiescent cells. The $[Ca^{2+}]_i$ increase in non-activated myofibroblasts stimulated with 100 nM ET-1 was ten times greater than that in activated myofibroblasts (Figure 2b). The increased $[Ca^{2+}]_i$ was suppressed by pretreatment of the cells with 3 μM BQ-123, indicating that the $[Ca^{2+}]_i$ increase was mediated mainly through the ET_A receptor (Figure 2d). Sarafotoxin S6c (100 nM), a selective ET_B receptor agonist, did not increase $[Ca^{2+}]_i$ either in quiescent or in activated myofibroblasts ($n = 4$ each). On the other hand, quiescent myofibroblasts did not respond to 10 ng ml^{-1} PDGF-BB, while PDGF-BB induced a sustained $[Ca^{2+}]_i$ increase in activated myofibroblasts (Figure 2c).

We next analysed the source of Ca^{2+} responsible for the increase in $[Ca^{2+}]_i$. In both the quiescent and activated cells, 10 μM ATP, 100 nM ET-1 and 10 ng ml^{-1} PDGF-BB all induced transient increases in $[Ca^{2+}]_i$ when stimulated in a Ca^{2+}-free solution containing 0.5 mM EGTA, but the sustained increases in $[Ca^{2+}]_i$ due to these agonists (AUC 3–4 min) were completely abolished (Figure 3). Therefore, there are two pathways which causes the $[Ca^{2+}]_i$ increase; Ca^{2+} release from intracellular Ca^{2+} stores, which is represented by the

transient increase in $[Ca^{2+}]_i$, and influx of extracellular Ca^{2+} through channels, which is represented by the sustained increases in $[Ca^{2+}]_i$.

The transient increases in $[Ca^{2+}]_i$ stimulated by 10 μM ATP, 100 nM ET-1 and 10 ng ml^{-1} PDGF-BB, in both quiescent and activated cells, and the sustained increases in $[Ca^{2+}]_i$ in quiescent cells were unaffected by pretreatment with 100 nM nicardipine, a voltage-dependent Ca^{2+} channel blocker (Figure 4a–d). However, in the activated cells, the sustained increases in $[Ca^{2+}]_i$ induced by 10 μM ATP and 10 ng ml^{-1} PDGF-BB were partly and significantly inhibited in the presence of nicardipine (Figure 4c and d).

$[Ca^{2+}]_i$ responses to Bay K8644 and membrane depolarization due to high concentration of K^+

Myofibroblasts were stimulated with either Bay K8644 (1 μM) or with a high concentration of K^+ (72.4 mM) to further investigate the involvement of voltage-dependent Ca^{2+} channels in raising $[Ca^{2+}]_i$. Both Bay K8644 (1 μM) (AUC: 0–3 min) and a high concentration of K^+ (72.4 mM) (AUC: 0–2 min) induced sustained increases in $[Ca^{2+}]_i$ which were more than twofold greater in activated cells than in quiescent cells (Figure 5a–d). Stimulation with either Bay K8644 or high K^+ raised the $[Ca^{2+}]_i$ a few hundred nanomolar higher than the resting level. The sustained increases in $[Ca^{2+}]_i$ activated cells induced by a high concentration of K^+ (72.4 mM) was significantly reduced when cells were pretreated with nicardipine (100 nM) for 3 min (Figure 5e and f). From these results, it can be concluded that external Ca^{2+} influx contributes to the sustained components of Ca^{2+} responses, where voltage-dependent Ca^{2+} channels take a part in activated myofibroblasts.
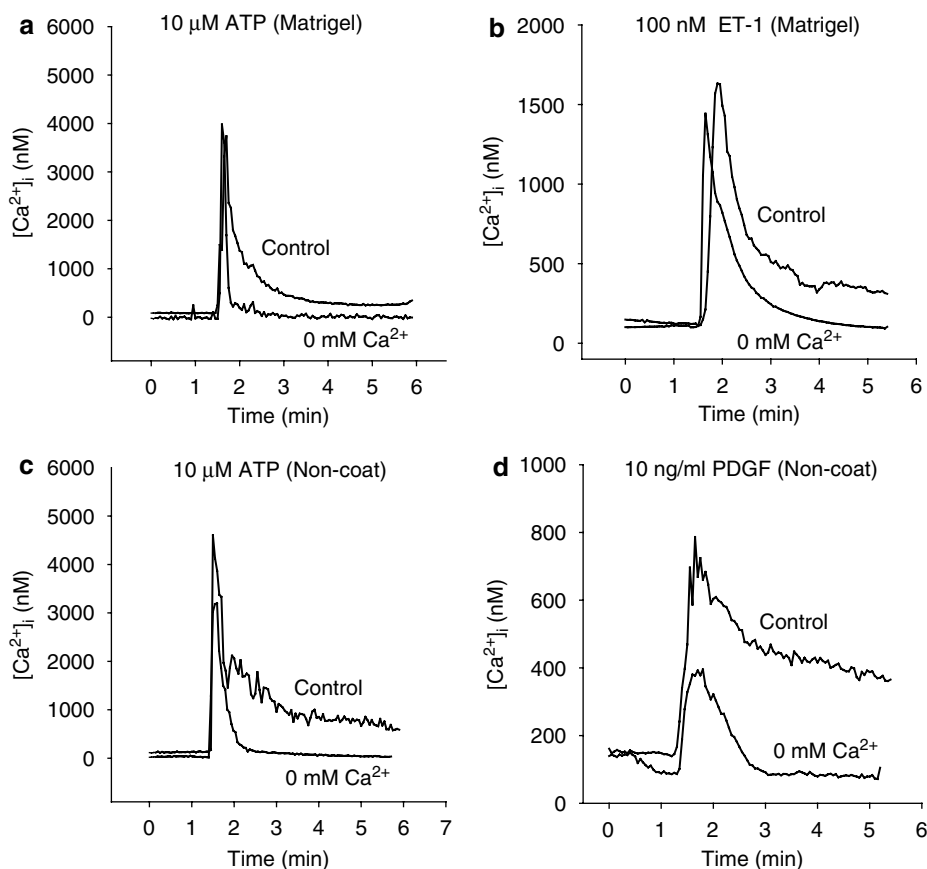
Figure 3 Ca^{2+} sources responsible for the increase in intracellular Ca^{2+} concentration ($[Ca^{2+}]_i$) due to 10 μM adenosine 5'-triphosphate (ATP), 100 nM endothelin-1 (ET-1) and 10 ng ml^{-1} platelet-derived growth factor-BB (PDGF-BB) in myofibroblasts cultured on either Matrigel (**a** and **b**) or non-coated plastic dish (**c** and **d**). Myofibroblasts were stimulated with either 10 μM ATP, 100 nM ET-1, or with 10 ng ml^{-1} PDGF-BB in a Ca^{2+}-free solution containing 0.5 mM ethylene glycol bis(β-aminoethylether)-*N,N,N',N'*,-tetraacetic acid (EGTA). The media was changed to a Ca^{2+}-free solution containing 0.5 mM EGTA 30 s before addition of each agonist.

Analysis of store-operated Ca^{2+} influx by depletion of Ca^{2+} store with thapsigargin

We then questioned whether store-operated Ca^{2+} influx pathways contribute to the nicardipine-insensitive Ca^{2+} influx. Therefore, we depleted the Ca^{2+} stores by treatment with thapsigargin (3 μM) in a Ca^{2+}-free solution with 0.5 mM EGTA. After 4 min, the addition of 1.5 mM Ca^{2+} induced a sustained increase in $[Ca^{2+}]_i$ in activated and quiescent cells. In contrast to the responses to Bay K8644 and high K^+, the increase in $[Ca^{2+}]_i$ due to addition of Ca^{2+} in the cells cultured on Matrigel was comparable to non-coated plastic-cultured cells (AUC: 0–3 min) (Figure 6b). The addition of 2-APB (10 μM) and Gd^{3+} (10 μM), inhibitors of store-operated Ca^{2+} influx, suppressed the sustained $[Ca^{2+}]_i$ increase to resting level after 1–2 min in the cells cultured on Matrigel and non-coated plastic dishes ($n=4$ each).

Expression of prepro ET-1, PDGF-A and PDGF-B

PreproET-1, PDGF-A and PDGF-B transcripts were compared between cells cultured in Matrigel and on non-coated plastic. Activated myofibroblasts expressed a significantly greater amount of prepro ET-1 than quiescent myofibroblasts (Figure 7). There was no significant difference between

PDGF-A and PDGF-B expression between the quiescent and activated cells (Figure 7). In both quiescent and activated cells, expression of PDGF-A was higher than PDGF-B expression.

Expression of ET_A, PDGFR-α and PDGFR-β

PreproET$_A$, PDGFR-α and PDGFR-β transcripts were compared between Matrigel and non-coated plastic-cultured cells. Quiescent myofibroblasts expressed a significantly greater amount of ET$_A$ than activated myofibroblasts (Figure 8). On the other hand, there was no significant difference between PDGFR-α and PDGFR-β expression between the quiescent and activated cells.

Discussion

Culture of fibroblasts, myofibroblasts or HSCs on plastic in an unnatural two-dimensional (2D) environment imitates injury and leads to a spontaneous activation to a fibrogenic phenotype. Transfer of these cells into a 3D environment (contractable collagen gel) returns the cells to a quiescent phenotype (Friedman *et al.*, 1989; Senoo *et al.*, 1996;
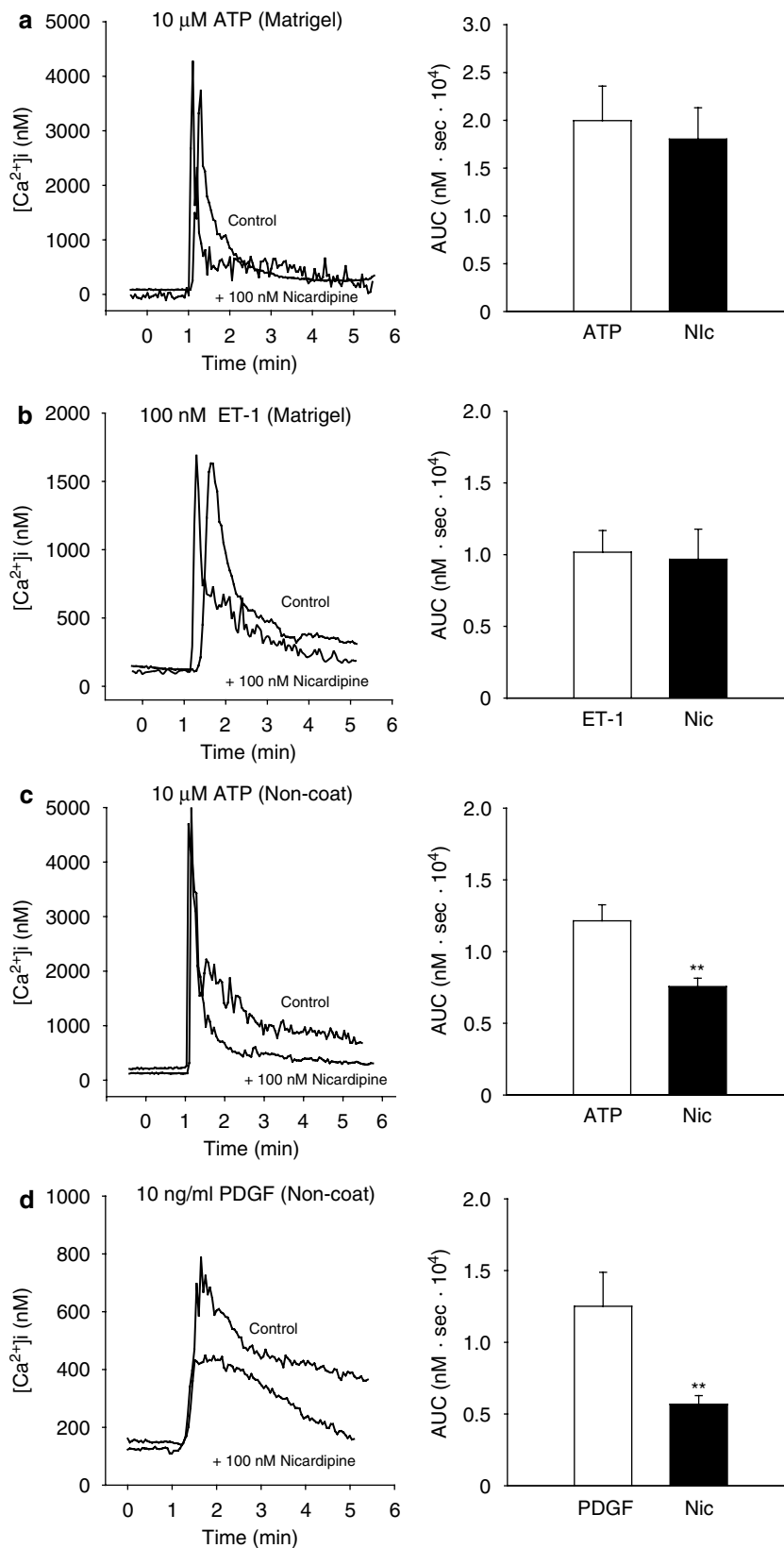
Figure 4 Effect of nicardipine on the increase in intracellular Ca^{2+} concentration ($[Ca^{2+}]_i$) due to $10\,\mu M$ adenosine $5'$-triphosphate (ATP), $100\,nM$ endothelin-1 (ET-1) and $10\,ng\,ml^{-1}$ platelet-derived growth factor-BB (PDGF-BB) in myofibroblasts cultured on either Matrigel (**a** and **b**) or non-coated plastic dish (**c** and **d**). Results are shown as the area under the $[Ca^{2+}]_i$-time curve (AUC: 3–4 min). Myofibroblasts were pretreated with $100\,nM$ nicardipine for 3 min before stimulation with these agonists. Data are presented as the mean $\pm$ s.e.m. of 13–40 cells from 4 separate experiments. $**P < 0.01$.
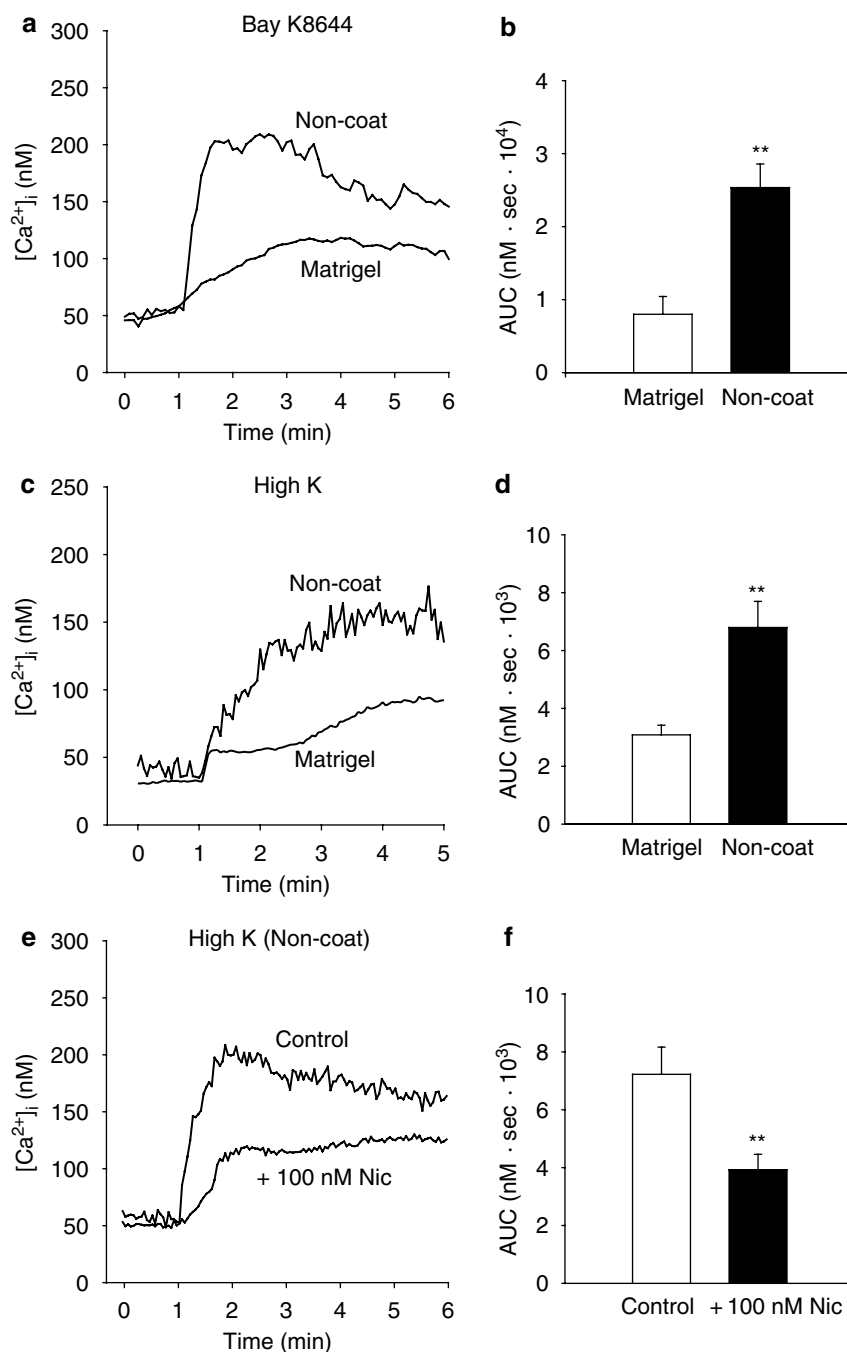
Figure 5 Effect of Bay K8644 (1 μM) and a high concentration of K (72.4 mM) on intracellular Ca^{2+} concentration ($[Ca^{2+}]_i$) on myofibroblasts cultured on either Matrigel or non-coated plastic dishes. Myofibroblasts were stimulated with Bay K8644 (1 μM) (**a** and **b**) or with a high concentration of K^+ (72.4 mM) (**c** and **d**). (**e** and **f**) Activated myofibroblasts were pretreated with nicardipine (100 nM) for 3 min before stimulation with high K^+. Results are shown as the area under the $[Ca^{2+}]_i$-time curve (**b**: AUC: 0–3 min) (**d** and **f**: AUC: 0–2 min). Data are presented as mean$\pm$s.e.m. of 17–38 cells from 4 separate experiments. **$P<0.01$.

Schuppan and Porov, 2002; Sohara *et al.*, 2002). From the difference in expression of α-SMA in protein and mRNA levels, it was clear that rat liver myofibroblasts cultured on Matrigel and non-coated plastic dishes could be used as quiescent and activated models of myofibroblasts, respectively (Figure 1). The shape of the cell cultured on a collagen-(cell matrix collagen Type I-A, Nitta Gelatin) coated dish did not differ from that of the cells cultured on a non-coated dish; that is, they were spread out and flattened similar to the non-coated plastic-cultured cells. Using cells cultured on collagen-coated dish, we investigated the response to ET-1 and PDGF-BB in these cells. Cells cultured in this way showed almost no response to ET-1 and, in turn, a significant $[Ca^{2+}]_i$ increase in response to PDGF-BB (data not shown). These results were comparable to that of cells cultured on non-coated plastic dishes. Therefore, it can be concluded
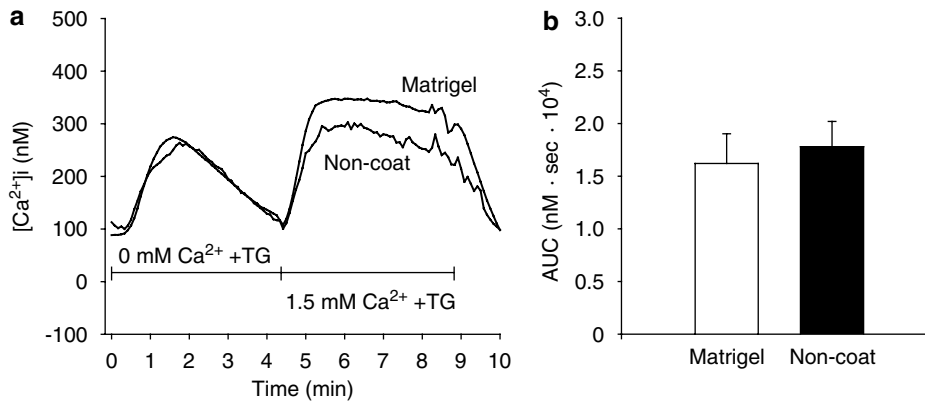
Figure 6 Involvement of store-operated Ca^{2+} influx. Myofibroblasts cultured on either Matrigel or non-coated plastic were stimulated with 3 μM thapsigargin in a Ca^{2+}-free solution containing 0.5 mM ethylene glycol bis(β-aminoethylether)-*N,N,N′,N′*,-tetraacetic acid (EGTA). After 4 min, the medium was changed to 1.5 mM Ca^{2+} solution (**a**). (**b**) The area under the intracellular Ca^{2+} concentration ([Ca^{2+}]$_i$)–time curve after the medium was changed to a 1.5 mM Ca^{2+} solution (AUC: 0–3 min). Data are presented as mean$\pm$s.e.m. of 15–31 cells from 4 separate experiments.
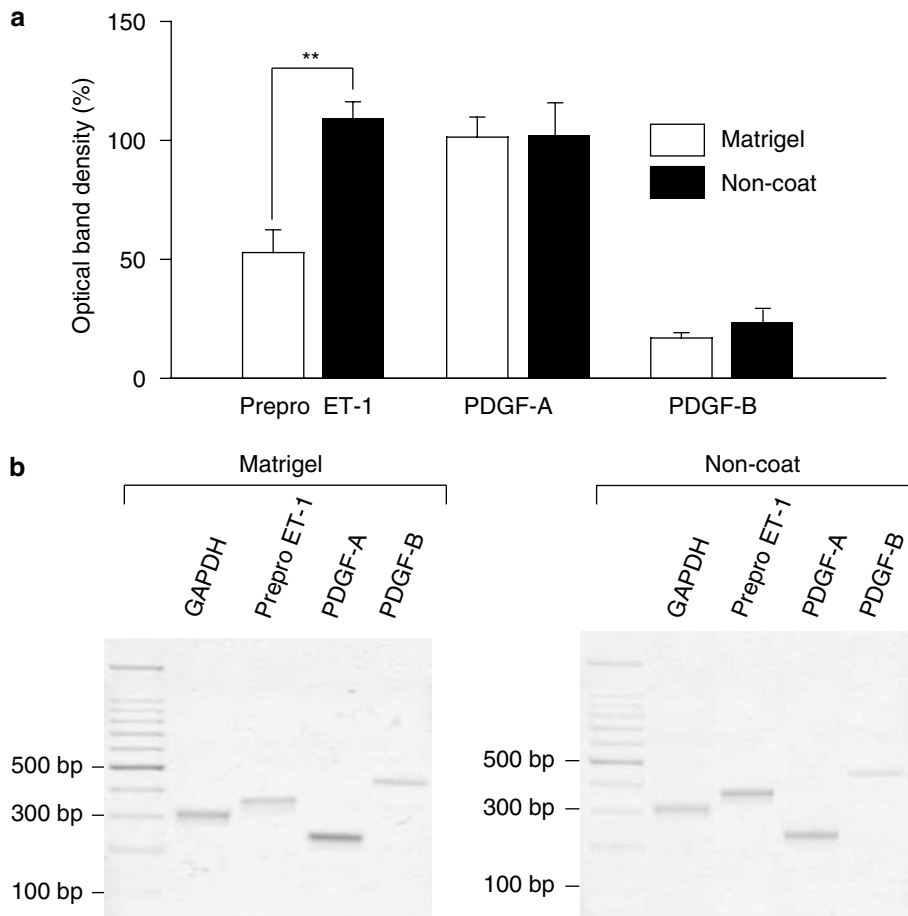

Figure 7 Expressions of prepro endothelin-1 (ET-1), platelet-derived growth factor-A (PDGF-A) and PDGF-B in quiescent and activated myofibroblasts. Myofibroblasts were cultured on either Matrigel or non-coated plastic dishes and starved overnight. Expression of prepro ET-1, PDGF-A and PDGF-B mRNA was analysed by reverse-transcription polymerase chain reaction (RT-PCR). (**a**) Results are expressed as the percentage of optical density$\pm$s.e.m. relative to glyceraldehyde-3-phosphate dehydrogenase (GAPDH). **P<0.01 (*n* = 5–6). (**b**) Typical trace of RT-PCR analysis for GAPDH, prepro ET-1, PDGF-A and PDGF-B.

that it was not the components of the collagen that induced the phenotypical change, but the contractable gel medium, as shown previously (Friedman *et al.*, 1989). We believe that

the Matrigel-cultured cells reflect the quiescent myofibro-blasts, which are located around the portal tract and the central vein. In comparison, the non-coated plastic-cultured
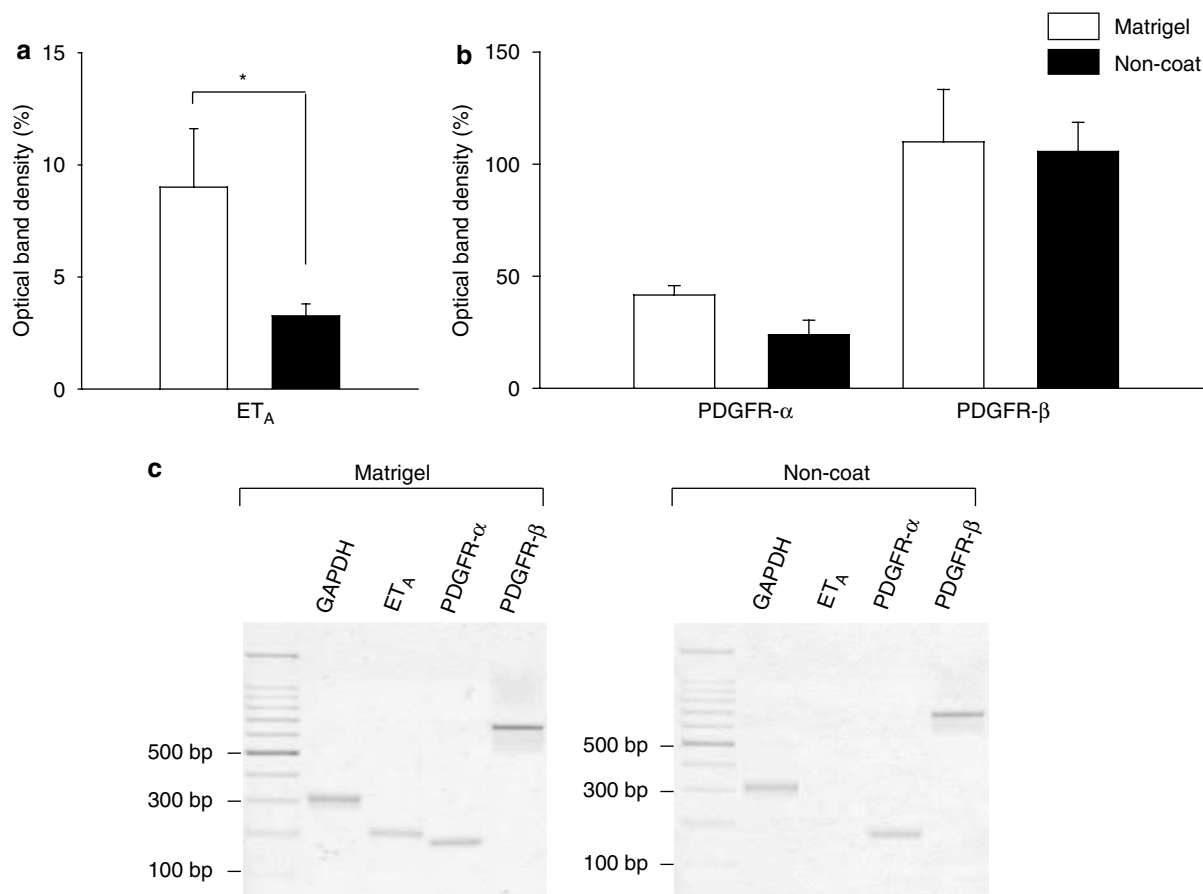
Effect of ET-1 and PDGF on liver myofibroblasts
N Kojima et al
825

Figure 8 Expressions of endothelin A (ET_A), platelet-derived growth factor receptor-α (PDGFR-α) and PDGFR-β in quiescent and activated myofibroblasts. Myofibroblasts were cultured on either Matrigel or non-coated plastic dishes and starved overnight. Expression of ET_A, PDGFR-α and PDGFR-β mRNA was analysed by reverse-transcription polymerase chain reaction (RT-PCR). (**a** and **b**) Results are expressed as the percentage of optical density $\pm$ s.e.m. relative to GAPDH. *$P < 0.05$ ($n = 6$–7). (**c**) Typical trace of RT-PCR analysis for GAPDH, ET_A, PDGFR-α and PDGFR-β.

cells reflect the activated myofibroblasts which proliferate and migrate around the fibrosing areas of the liver (Ramadori and Saile, 2002). In this study, we evaluated fibrogenic activity using these two types of cells; Matrigel- or non-coated plastic-cultured cells, by analysing the change in $[Ca^{2+}]_i$.

$[Ca^{2+}]_i$ acts as a second messenger in a variety of cells and regulates numerous cell functions, including movements, secretion, cell death and contraction. Abnormal contractions due to raised $[Ca^{2+}]_i$ in myofibroblasts in the liver can lead to liver stiffness and changes in microvascular circulation. Cell migration is also mediated and regulated via activation of a number of Ca^{2+}-dependent enzymes (Pauly et al., 1995; Yang and Huang, 2005) and the migration of myofibroblasts to the liver injury site contributes to the development of liver fibrosis. In vascular smooth muscles, it has recently been suggested that Ca^{2+} signals regulate smooth muscle cell-specific gene expression through RhoA/ROK/myocardin-, calcineurin/NFAT and Ca^{2+}/calmodulin-dependent protein kinase/P-CREB systems (Wamhoff et al., 2006), which may also contribute to the myofibroblast activation.

The most important finding of this study is that ET-1 induces a greater $[Ca^{2+}]_i$ increase in quiescent than in activated myofibroblasts, while PDGF-BB induces a greater $[Ca^{2+}]_i$ increase in activated than in quiescent myofibro-

blasts. The results of the present study also demonstrate that the sensitivity of myofibroblasts to produce a $[Ca^{2+}]_i$ response to ATP does not change during the activation process, indicating that the Ca^{2+} signalling mechanism per se is not greatly altered after the phenotypic conversion to myofibroblasts, rich in α-SMA.

In normal liver, ET-1 is thought to participate in regulating microcirculation and physiological collagen synthesis (Gandhi et al., 2000). In liver fibrosis, ET-1 is upregulated and released from activated sinusoidal endothelium and HSCs, leading to autocrine and paracrine activation (Pinzani et al., 1996; Rockey et al., 1998; Friedman, 2000). Receptor types A (ET_A) and B (ET_B) are expressed on both quiescent and activated cells (Kawada et al., 1995), but upon early activation, ET_A receptor sensitivity is increased in HSCs (Reinehr et al., 1998). With full HSC activation, a shift in the relative prevalence of ET_A to the ET_B receptors is observed (Pinzani et al., 1996). While stimulation of ET_A receptors with ET-1 in HSCs increases $[Ca^{2+}]_i$ (Guo et al., 2004), stimulates proliferation through a Ras/ERK pathway (Pinzani et al., 1996) and induces contraction (Kawada et al., 1995; Thimgan and Yee, 1999), stimulation of ET_B receptors with ET-1 mediates growth inhibitory effects through a prosta-glandin/cAMP pathway (Mallat et al., 1996). Our findings for

ET signalling in the liver myofibroblasts were essentially similar to those of HSCs; that is, (1) Ca^{2+} mobilization was mainly mediated through the ET_A receptor, (2) the ET-1-induced increase in $[Ca^{2+}]_i$ was diminished after myofibroblastic activation, which may be attributable to the down-regulation of ET_A receptors and (3) prepro ET-1 was upregulated upon myofibroblastic activation. In quiescent liver myofibroblasts, stimulation of ET_A receptors with upregulated ET-1 increased $[Ca^{2+}]_i$, and may have stimulated some properties such as proliferation in HSCs, but this mechanism did not persist for a long period and diminished with activation.

On the other hand, PDGF is the best characterized and the most potent proliferative factor in hepatic fibrosis. The present results clearly demonstrate that quiescent liver myofibroblasts did not respond to PDGF-BB until myofibroblastic conversion, indicating the presence of transdifferentiation-dependent sensitization of liver myofibroblasts toward PDGF-BB. PDGFR-β seems to be the dominant receptor type consistent with previous observations suggesting that PDGF-BB and its receptors play an important role in liver fibrosis (Friedman, 2000; Czochra et al., 2006). The present investigation further showed no difference in mRNA expression of PDGFR-α or PDGFR-β between Matrigel- and plastic-cultured myofibroblasts, indicating that signal transduction pathways after PDGF receptor stimulation may have been upregulated in the activated cells. Further investigations are needed to clarify the underlying mechanisms.

In the present study, we analysed the Ca^{2+} source responsible for the increase in $[Ca^{2+}]_i$. All the fibrogenic agents tested were capable of inducing a transient increase in $[Ca^{2+}]_i$ even in the absence of external Ca^{2+}, indicating the involvement of Ca^{2+} release from cellular stores at the initial phase. As for the sustained phase, nicardipine inhibited the ATP-induced increase in $[Ca^{2+}]_i$ in the activated cells, but not in quiescent cells. The PDGF-BB-induced increase in $[Ca^{2+}]_i$ in the activated cells, but not the ET-1-induced increase in $[Ca^{2+}]_i$ in quiescent cells, was also partly inhibited by nicardipine. Moreover, Bay K8644 and a high concentration of K^+ induced sustained increases in $[Ca^{2+}]_i$ that were significantly greater in activated cells than in quiescent cells. Therefore, voltage-dependent L-type Ca^{2+} channels were involved in the agonist-induced Ca^{2+} influx at the sustained $[Ca^{2+}]_i$ phase in activated cells but not in quiescent cells. These results obtained with liver myofibroblasts are consistent with electrophysiological data obtained from HSCs; that is, activation of HSCs is associated with upregulation of voltage-dependent L-type Ca^{2+} channels that mediate Ca^{2+} influx and cell contraction (Roth-Eichhorn et al., 1999; Bataller et al., 2001). Moreover, from the analysis of the effect of Ca^{2+} store depletion on Ca^{2+} influx, we found that the nicardipine-insensitive Ca^{2+} influx in the sustained $[Ca^{2+}]_i$ phase should be attributable to 2-APB- and Gd^{3+}-sensitive store-operated Ca^{2+} influx pathways. Also, the store-operated Ca^{2+} influx was comparable between Matrigel- and non-coated plastic-cultured cells; and thus unlike the nicardipine-sensitive voltage-dependent Ca^{2+} channels which were upregulated in the activated cells, there was no transdifferentiation-dependent upregulation for this Ca^{2+} influx pathway.

In summary, the profiles of changes in $[Ca^{2+}]_i$ due to ET-1 and PDGF were different in quiescent and activated liver myofibroblasts. It may be that ET-1 plays an important role in the process of wound healing (contraction) or cell migration at the early stage of liver fibrosis and that PDGF may contribute mainly to myofibroblast proliferation at the late stage of liver fibrosis. Although Ca^{2+} plays important physiological roles in the myofibroblast fibrogenic response, studies of Ca^{2+} signalling in response to factors that contribute to liver fibrosis have not been adequate. ET_A receptor antagonists and drugs which inhibit the PDGF response and also drugs that inhibit L-type Ca^{2+} channels and store-operated Ca^{2+} channels can be expected to be potential antifibrotic therapy for liver fibrosis. The present results may provide a better understanding of the process of liver fibrosis and new insights into the development of a pharmacological therapeutic strategy targeting ET and PDGF.

Acknowledgements

Conflict of interest

The authors state no conflict of interest.

References

Bataller R, Brenner DA (2005). Liver fibrosis. J Clin Invest 115: 209–218.

Bataller R, Gasull X, Gines P, Hellemans K, Gorbig MN, Nicolas JM et al. (2001). In vitro and in vivo activation of rat hepatic stellate cells results in de novo expression of L-type voltage-operated calcium channels. Hepatology 33: 956–962.

Carpino G, Morini S, Ginanni Corradini S, Franchitto A, Merli M, Siciliano M et al. (2005). α-SMA expression in hepatic stellate cells and quantitative analysis of hepatic fibrosis in cirrhosis and in recurrent chronic hepatitis after liver transplantation. Dig Liver Dis 37: 349–356.

Czochra P, Klopcic B, Meyer E, Herkel J, Garcia-Lazaro JF, Thieringer F et al. (2006). Liver fibrosis induced by hepatic overexpression of PDGF-B in transgenic mice. J Hepatol 45: 419–428.

Desmouliere A, Darby IA, Gabbiani G (2003). Normal and pathologic soft tissue remodeling: role of the myofibroblast, with special emphasis on liver and kidney fibrosis. Lab Invest 83: 1689–1707.

Dranoff JA, Ogawa M, Kruglov EA, Gaca MD, Sevigny J, Robson SC et al. (2004). Expression of P2Y nucleotide receptors and ectonucleotidases in quiescent and activated rat hepatic stellate cells. Am J Physiol Gastrointest Liver Physiol 287: G417–G424.

Friedman SL (2000). Molecular regulation of hepatic fibrosis, an integrated cellular response to tissue injury. J Biol Chem 275: 2247–2250.

Friedman SL, Roll FJ, Boyles J, Arenson DM, Bissell DM (1989). Maintenance of differentiated phenotype of cultured rat hepatic lipocytes by basement membrane matrix. J Biol Chem 264: 10756–10762.

Gandhi CR, Kuddus RH, Uemura T, Rao AS (2000). Endothelin stimulates transforming growth factor-beta1 and collagen synthesis in stellate cells from control but not cirrhotic rat liver. Eur J Pharmacol 406: 311–318.

Guo CY, Wu JY, Wu YB, Zhong MZ, Lu HM (2004). Effects of endothelin-1 on hepatic stellate cell proliferation, collagen synthesis and secretion, intracellular free calcium concentration. World J Gastroenterol 10: 2697–2700.

Harada H, Chan CM, Loesch A, Unwin R, Burnstock G (2000). Induction of proliferation and apoptotic cell death via P2Y and P2X receptors, respectively, in rat glomerular mesangial cells. *Kidney Int* **57**: 949–958.

Hui AY, Friedman SL (2003). Molecular basis of hepatic fibrosis. *Expert Rev Mol Med* **2003**: 1–23.

Kawada N, Kuroki T, Kobayashi K, Inoue M, Kaneda K, Decker K (1995). Action of endothelins on hepatic stellate cells. *J Gastroenterol* **30**: 731–738.

Kinnman N, Francoz C, Barbu V, Wendum D, Rey C, Hultcrantz R et al. (2003). The myofibroblastic conversion of peribiliary fibrogenic cells distinct from hepatic stellate cells is stimulated by platelet-derived growth factor during liver fibrogenesis. *Lab Invest* **83**: 163–173.

Kinnman N, Goria O, Wendum D, Gendron MC, Rey C, Poupon R et al. (2001). Hepatic stellate cell proliferation is an early platelet-derived growth factor-mediated cellular event in rat cholestatic liver injury. *Lab Invest* **81**: 1709–1716.

Kinnman N, Hultcrantz R, Barbu V, Rey C, Wendum D, Poupon R et al. (2000). PDGF-mediated chemoattraction of hepatic stellate cells by bile duct segments in cholestatic liver injury. *Lab Invest* **80**: 697–707.

Knittel T, Kobold D, Saile B, Grundmann A, Neubauer K, Piscaglia F et al. (1999). Rat liver myofibroblasts and hepatic stellate cells: different cell populations of the fibroblast lineage with fibrogenic potential. *Gastroenterology* **117**: 1205–1221.

Mallat A, Preaux AM, Serradeil-Le Gal C, Raufaste D, Gallois C, Brenner DA et al. (1996). Growth inhibitory properties of endothelin-1 in activated human hepatic stellate cells: a cyclic adenosine monophosphate-mediated pathway. Inhibition of both extracellular signal-regulated kinase and c-Jun kinase and upregulation of endothelin B receptors. *J Clin Invest* **98**: 2771–2778.

Muddu AK, Guha IN, Elsharkawy AM, Mann DA (2007). Resolving fibrosis in the diseased liver: translating the scientific promise to the clinic. *Int J Biochem Cell Biol* **39**: 695–714.

Novo E, Marra F, Zamara E, Valfre di Bonzo L, Caligiuri A, Cannito S et al. (2006). Dose dependent and divergent effects of superoxide anion on cell death, proliferation, and migration of activated human hepatic stellate cells. *Gut* **55**: 90–97.

Olaso E, Friedman SL (1998). Molecular regulation of hepatic fibrogenesis. *J Hepatol* **29**: 836–847.

Pauly RR, Bilato C, Sollott SJ, Monticone R, Kelly PT, Lakatta EG et al. (1995). Role of calcium/calmodulin-dependent protein kinase II in the regulation of vascular smooth muscle cell migration. *Circulation* **91**: 1107–1115.

Pinzani M, Rombouts K (2004). Liver fibrosis: from the bench to clinical targets. *Dig Liver Dis* **36**: 231–242.

Pinzani M, Gesualdo L, Sabbah GM, Abboud HE (1989). Effects of platelet-derived growth factor and other polypeptide mitogens on DNA synthesis and growth of cultured rat liver fat-storing cells. *J Clin Invest* **84**: 1786–1793.

Pinzani M, Milani S, De Franco R, Grappone C, Caligiuri A, Gentilini A et al. (1996). Endothelin 1 is overexpressed in human cirrhotic liver and exerts multiple effects on activated hepatic stellate cells. *Gastroenterology* **110**: 534–548.

Ramadori G, Saile B (2002). Mesenchymal cells in the liver – one cell type or two? *Liver* **22**: 283–294.

Ramadori G, Saile B (2004). Portal tract fibrogenesis in the liver. *Lab Invest* **84**: 153–159.

Reinehr R, Fischer R, Haussinger D (2002). Regulation of endothelin-A receptor sensitivity by cyclic adenosine monophosphate in rat hepatic stellate cells. *Hepatology* **36**: 861–873.

Reinehr RM, Kubitz R, Peters-Regehr T, Bode JG, Haussinger D (1998). Activation of rat hepatic stellate cells in culture is associated with increased sensitivity to endothelin 1. *Hepatology* **28**: 1566–1577.

Reynaert H, Thompson MG, Thomas T, Geerts A (2002). Hepatic stellate cells: role in microcirculation and pathophysiology of portal hypertension. *Gut* **50**: 571–581.

Rockey DC, Fouassier L, Chung JJ, Carayon A, Vallee P, Rey C et al. (1998). Cellular localization of endothelin-1 and increased production in liver injury in the rat: potential for autocrine and paracrine effects on stellate cells. *Hepatology* **27**: 472–480.

Roth-Eichhorn S, Eberheim A, Bode HP, Gressner AM (1999). Transformation-dependent calcium influx by voltage-operated calcium channels in stellate cells of rat liver. *J Hepatol* **30**: 612–620.

Saile B, Matthes N, Neubauer K, Eisenbach C, El-Armouche H, Dudas J et al. (2002). Rat liver myofibroblasts and hepatic stellate cells differ in CD95-mediated apoptosis and response to TNF-α. *Am J Physiol Gastrointest Liver Physiol* **283**: G435–G444.

Schuppan D, Porov Y (2002). Hepatic fibrosis: from bench to bedside. *J Gastroenterol Hepatol* **17** (Suppl 3): S300–S305.

Senoo H, Imai K, Sato M, Kojima N, Miura M, Hata R (1996). Three-dimensional structure of extracellular matrix reversibly regulates morphology, proliferation and collagen metabolism of perisinusoidal stellate cells (vitamin A-storing cells). *Cell Biol Int* **20**: 501–512.

Sohara N, Znoyko I, Levy MT, Trojanowska M, Reuben A (2002). Reversal of activation of human myofibroblast-like cells by culture on a basement membrane-like substrate. *J Hepatol* **37**: 214–221.

Tangkijvanich P, Melton AC, Chitapanarux T, Han J, Yee HF (2002). Platelet-derived growth factor-BB and lysophosphatidic acid distinctly regulate hepatic myofibroblast migration through focal adhesion kinase. *Exp Cell Res* **281**: 140–147.

Tangkijvanich P, Tam SP, Yee Jr HF (2001). Wound-induced migration of rat hepatic stellate cells is modulated by endothelin-1 through rho-kinase-mediated alterations in the acto-myosin cytoskeleton. *Hepatology* **33**: 74–80.

Thimgan MS, Yee Jr HF (1999). Quantitation of rat hepatic stellate cell contraction: stellate cells' contribution to sinusoidal resistance. *Am J Physiol* **277**: G137–G143.

Wamhoff BR, Bowles DK, Owens GK (2006). Excitation-transcription coupling in arterial smooth muscle. *Circ Res* **98**: 868–878.

Yang S, Huang XY (2005). Ca^{2+} influx through L-type Ca^{2+} channels controls the trailing tail contraction in growth factor-induced fibroblast cell migration. *J Biol Chem* **280**: 27130–27137.